Journal of Nuclear Materials 385 (2009) 479–484

Contents lists available at ScienceDirect

Journal of Nuclear Materials

journal homepage: www.elsevier.com/locate/jnucmat

Luminescent monitoring of metal dititanium triphosphates as promising materials for radioactive waste confinement

S. Nedilko [a], Yu. Hizhnyi [a,*], O. Chukova [a], P. Nagornyi [a], R. Bojko [b], V. Boyko [b]

[a] Kyiv National Taras Shevchenko University, 2, Block 1, Hlushkov Ave., 03680 Kyiv, Ukraine
[b] National Agriculture University, 5, Geroiv Oborony St., 03041 Kyiv, Ukraine

ARTICLE INFO

PACS:
78.55.Hx
78.20.Ci
28.41.Kw

ABSTRACT

The potential use of luminescent probes for control over the structural state of $MTi_2(PO_4)_3$ double metal phosphates as host materials for radioactive waste confinement is examined. Luminescence spectra of pure and metal (Al, In, V) and rare-earth (Pr, Sm, Dy) doped $MTi_2(PO_4)_3$ (M = Li, Na, K) phosphate compounds (in crystalline and related amorphous forms) under X-ray, VUV (synchrotron radiation), UV and visible light excitations are analyzed. Electronic structure and absorption spectra of $NaTi_2(PO_4)_3$ crystals are calculated by the full-potential LAPW method. The origin of the self and impurity emission bands of $MTi_2(PO_4)_3$ materials is defined. It was shown that nitrogen laser with 337.1 nm generation wavelength is the most effective excitation source for remote monitoring of incorporation of various types of waste elements into $MTi_2(PO_4)_3$ hosts and for control over states of these hosts during storage of radioactive waste.

1. Introduction

The alkaline and other metal (titanium or zirconium) phosphates like $M^{I}TiOPO_4$, $M^{I}(Ti,Zr)_2(PO_4)_3$ (M^{I} = Li, Na, K) are known as materials suitable for incorporation of radioactive waste over geological time scales [1,2]. Owing to peculiarities of their crystal structure and the presence of cations with different charges, these materials are able to incorporate chemical elements from different groups of the Periodic Table: from singly-charged cations of alkali metals (Li^+, Na^+, K^+, ...) to multiply-charged cations of transition (Cr^{3+}, V^{4+}, ...) and rare-earth (Pr^{3+}, Sm^{3+}, Dy^{3+}, Nd^{3+}, ...) elements.

Incorporated elements have to disturb the lattice of the host crystal. The crystal structure may also be destroyed by radiation damage arising from the incorporated species. At the same time, the ability to incorporate a specific element, the maximum concentration and the type of lattice disturbance require investigation for each element being incorporated.

The use of luminescent probes is a well-known method of control over structural state of a solid material. In this work, we examine the possibility of use of the luminescent probe method in the case of $M^{I}Ti_2(PO_4)_3$ (M^{I} = Li, Na, K) phosphate materials. Preliminary results on this problem have been published [3–6].

The initial host material can undergo a variety of structural changes under radioactive irradiation during waste conservation. However, several important general trends can be outlined. If the initial host is a crystal, then amorphization can take place. On the other hand, if it is a glass, it can crystallize during storage. Therefore, analysis of changes in the luminescence characteristics of the material measured at different stages of storage can provide information on such structural transformations. It is evident that elaboration of such method of monitoring requires many years, and to reduce the time expenditure, in this work, we investigate characteristics of two extreme states of the host material, the crystal and the amorphous (glass) forms.

Measurements of the luminescence excitation and emission characteristics in themselves are insufficient to identify the structural changes. It is also necessary to know the nature of the luminescence processes and the influence of various factors on the luminescence characteristics of the confinement material. To determine the structure of the luminescence centres in $M^{I}Ti_2(PO_4)_3$ materials investigations were performed that included experimental measurements of luminescence under X-ray, synchrotron and optical excitations, along with theoretical calculations of the electronic structure and optical absorption spectra.

2. Details of experiments and calculations

The investigated compounds were obtained by the 'melting solution' method from the initial blend of M^{I}_2O–$M^{III}_2O_3$–P_2O_5–TiO_2 (M^{III} = In, Al, V, RE) common composition in 925–1325 K temperature region at ambient atmosphere conditions. Chemical interactions in M^{I}_2O–P_2O_5–TiO_2 system were studied by the method of isothermal saturation at 1125–1325 K and slow cooling of

* Corresponding author.
E-mail address: hizhnyi@univ.kiev.ua (Yu. Hizhnyi).

0022-3115/$ - see front matter © 2008 Elsevier B.V. All rights reserved.
doi:10.1016/j.jnucmat.2008.12.034

homogeneous fluxes to crystalline phase formation. The fluxes were held at the necessary temperature (975–1175 K) for at least 2 h until equilibrium between the liquid and solid phases was reached (it was proved by the chemical analysis that after 2 h of subsequent crystallization the composition of liquid phases was not changed). As a result, the synthesis of the double alkaline metal and titanium phosphates was made from melt solutions of the mentioned system.

When the crystallization process was finished, the residues of the liquid phases were poured out on a copper sheet for a fast cooling (more than 100 K min^{-1}) and vitrification (formation of the amorphous forms). The crystalline substances were washed off in dilute nitric acid, then in distillate water, and dried. The composition of the amorphous form was estimated approximately as 3.26 M^{I}_2O–2.41 P_2O_5–1 TiO_2.

The X-ray diffraction (XRD) phase analysis (*Cu* K_α-rays, scanning rate 2° min^{-1}) of products of M^{I}_2O–P_2O_5–TiO_2 system crystallization showed that $M^{I}Ti_2(PO_4)_3$ compounds were formed within a range of M^{I}_2O/P_2O_5 mole ratio from 0.72 to 1.40. The optimal value of the ratio was found to be 1.2. The resulting crystals were about $3 \times 5 \times 8$ mm in size.

Photoluminescence (PL) and PL excitation spectra of the samples were obtained at 4.2–300 K. The samples were placed into helium (or nitrogen) cryostats at low temperatures (4.2 and 77 K). Luminescence was excited by radiation from the following sources: the N_2-laser (excitation wavelength λ_{ex} = 337.1 nm), the Ar-laser (λ_{ex} = 476.5, 488.0 and 514.5 nm) and diode-pumped laser (λ_{ex} = 473 nm). The radiation from the powerful xenon lamp DKsL-1000 was also used for luminescence excitation. Radiation from the lamp was filtered using a prism monochromator DMR-4 (working region 200–700 nm, the average dispersion 1/40 mm $Å^{-1}$). The luminescence was registered using various spectrometers, which a cover wide spectral region: MDR-2 (working region 250–700 nm, average dispersion 1/20 mm $Å^{-1}$) and DFS-12 (420–830 nm and 1/5 mm $Å^{-1}$, respectively) diffraction spectrometers.

X-ray luminescence was excited using X-ray tube BSV-27 (Cu, 30 kV, 30 mA) in geometry of normal incidence of excitation beam with respect to the investigated sample. Registration of the X-ray-excited emission was done by MDR-2 monochromator in direction of 45° with respect to the excitation beam. Luminescence excitation and emission spectra were studied using synchrotron radiation in the energy region 3.5–20 eV. Experiments with synchrotron radiation were carried out on SUPERLUMI station at HASYLAB (DESY), Hamburg, Germany.

Calculations of the electronic structure of perfect $NaTi_2(PO_4)_3$ crystals were performed using the WIEN2k package in which the full-potential linear-augmented-plane-wave (FLAPW) method is implemented within the framework of density-functional theory (DFT) [7]. Sodium titanium triphosphate $NaTi_2(PO_4)_3$ crystal is characterized by space group #167 (R3-C) and lattice parameters $a = b = 8.4594$ Å, $c = 22.0668$ Å, $\alpha = \beta = 90°$, $\gamma = 120°$ [8]. The Perdew and Wang generalized gradient approximation was employed for the exchange-correlation potential [9]. Relativistic effects were treated in the scalar relativistic approximation. The muffin-tin (MT) radii R_{MT} were chosen as 2.15 and 1.89 a.u. for Na and Ti, respectively and 1.44 for P and O. The other important parameters of the method were chosen as the following, $l_{max} = 10$, $R_{MT}K_{max} = 6.0$, $G_{max} = 14.0$.

Partial densities of electronic states (PDOS) and the absorbance spectra k were calculated using well-known technique implemented in the WIEN2k package. Since the orientation of the crystal axes of the samples in experiments were not identified, the averaged spectra $k = (2k_x + k_z)/2$ (where k_x and k_z indicate absorbance calculated respectively for the x- and z-polarizations of the E vector of incident light) were used in analysis.

3. Results and discussion

Two bands are in general observed in emission spectra of $MTi_2(PO_4)_3$ crystals depending on the type and wavelength of exciting radiation. One broad band without a clearly expressed structure is observed in 350–700 nm spectral region (denoted here as LBI). In addition to this band, a narrower band (denoted as LBII) appears in the red spectral region, between 700 and 850 nm.

The X-ray luminescence spectrum of undoped $NaTi_2(PO_4)_3$ crystals at room temperature consist of two broad bands over whole region of visible light (Fig. 1, curve 1). The less intense short-wavelength emission band is located in region 460–700 nm with peak position near ~550 nm. The more intense long-wavelength (red) emission band in 720–800 nm region reaches the maximum near 760 nm. Under excitation by synchrotron radiation the short-wavelength emission band is shifted to higher energies reaching the peak position near 490 nm, whereas the red emission band of $NaTi_2(PO_4)_3$ crystals vanishes (Fig. 1, curve 2). The photoluminescence (PL) spectra of the crystals reveal the same two bands as in the case of X-ray luminescence (Fig. 1, curves 3–7). The red band is an order of magnitude more intense than the short-wavelength emission for all cases of laser excitations. Temperature changes cause redistribution between relative intensities of the short-wavelength and the red bands. Luminescence intensity of the first band essentially decreases with increasing temperature [10]. The luminescent band I (LBI) is obviously complex and, as the experiment shows, it is a superposition of at least three components with peak positions estimated at 430–440, 500–510 and 550–560 nm (Fig. 1).

Emission spectra of the phosphate crystals with another M^{I} cations are in general similar to the case of $NaTi_2(PO_4)_3$, however, the envelope of LBI band is slightly shifted due to changed contribution of different components into overall LBI emission. Ratio of the LBI

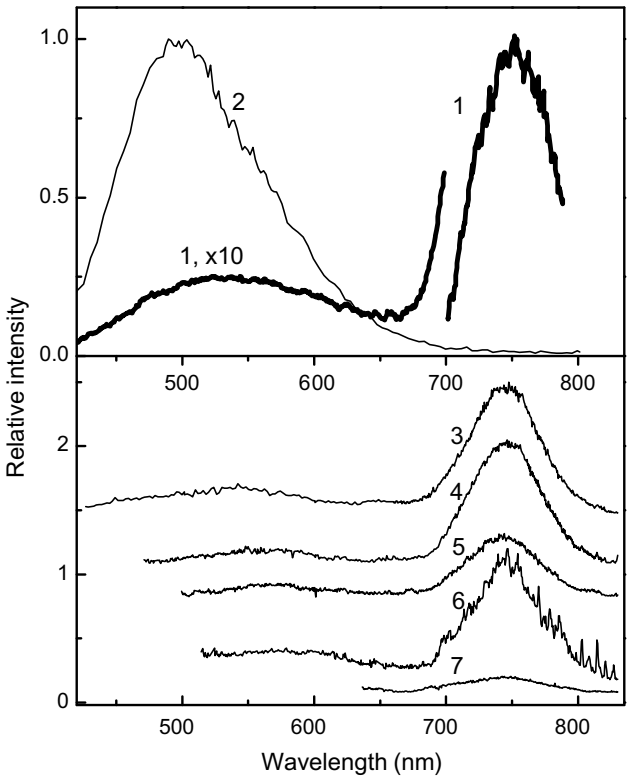

Fig. 1. Emission spectra of undoped $NaTi_2(PO_4)_3$ crystals measured under X-ray (1) synchrotron (2) and laser excitations (3–7); λ_{exc} = 170 (2), 337.1 (3), 457.9 (4), 488 (5), 496.5 (6) and 632.8 nm (7); T = 10 (2) and 300 K (1, 3–7).

and LBII intensities also depends on type of the cation (see Fig. 5 below).

Strong dependence of the luminescence characteristics on the type of excitation, excitation wavelength, temperature and crystal composition brings up the problem of choice of such excitation that should be the most effective for monitoring of composition and concentration of radioactive waste and structural state of the host matrix. This task also demands clarification of the origin of self emission of the host. For this purpose, experimental studies of the luminescence excitation spectra, as well as theoretical calculations of the electronic structure and absorption spectra were carried out.

PL excitation spectra of undoped $NaTi_2(PO_4)_3$ crystals reveal significant detail in the 250–500 nm region (Fig. 2, curves 1 and 2). The band with peak at 308 nm with the shoulders on high-energy side (at 302 and 295 nm) dominates in the excitation spectrum of the short-wavelength emission (curve 1). Several less intense bands with λ_{max} = 336, 401, 425 and 464 nm can also be seen in this curve. The LBII emission is excited in 250–545 nm region (curve 2). The peak positions of the main bands in this excitation spectrum are located near 475, 350 and 280 nm. As we can see, these bands in general correspond to the regions of excitation LBI band, but the region of the most effective excitation of LBI emission (280–330 nm) is absent here. Low-energy band at 475 nm is the most intensive band in the excitation spectrum of the LBII emission.

In order to clarify the origin of observed excitation and emission bands we carried out calculations of the electronic structure and optical spectra of perfect $NaTi_2(PO_4)_3$ crystals. Recently we studied the electronic structures and optical properties of several other phosphates using the same method of calculations [5,6]. Some important details of the calculation procedure and discussion on the determination of the energy gap of Ti-containing phosphate crystals can be found in our previous paper [11].

Calculated partial densities of electronic states (PDOS) of $NaTi_2(PO_4)_3$ crystal are presented in Fig. 3, where the origin of the energy scale is chosen at the Fermi level. Three clearly separated sub-bands characterize the conduction band (CB) of the crystal. These sub-bands lie between 2 and 3 eV, 4 and 5 eV, and above 6.5 eV. The first and the second of them are formed mainly by Ti *d* states, but with some content of O *p* states and significantly lower contribution of the P states. The O *p* states dominate in the upper part of the valence band (VB), where Ti *d* states contribute also. The electronic states of Na and P are situated mainly in the lower part of the valence band, from −9 to −4.5 eV and in the upper sub-band of the conduction band, above 6.5 eV.

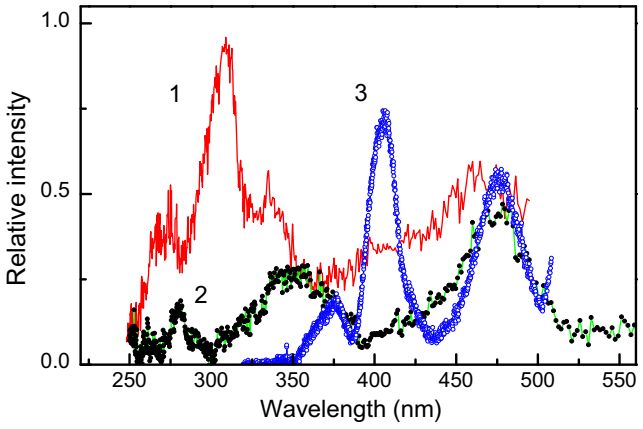

Fig. 2. Luminescence excitation spectra of undoped $NaTi_2(PO_4)_3$ crystals (1, 2) and crystals doped with Sm^{3+} ions (3); λ_{reg} = 530 (1), 770 (2) and 557 nm (3); *T* = 4.2 (1, 2) and 300 K (3).

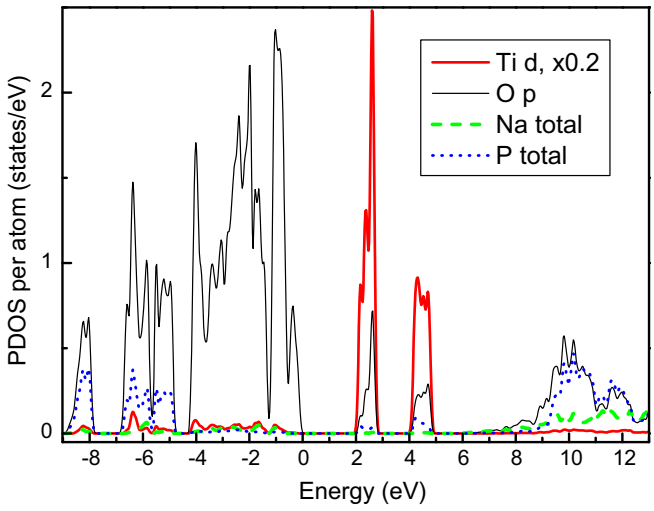

Fig. 3. Calculated partial densities of electronic states of $NaTi_2(PO_4)_3$ crystal.

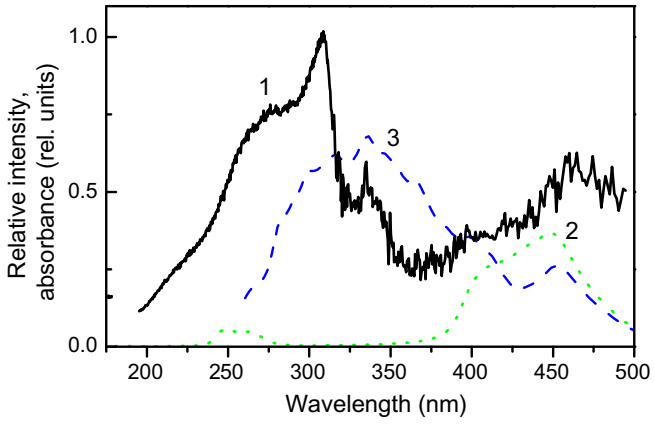

Fig. 4. Luminescence excitation spectra (1), λ_{reg} = 530 nm, *T* = 10 K, and calculated partial absorbance spectra k_1, k_2 (see text) of undoped $NaTi_2(PO_4)_3$ crystals (2, 3).

To study formation of the main peaks in the excitation spectra $NaTi_2(PO_4)_3$ crystals (Fig 4, curve 1) we carried out a decomposition of the interband absorption spectrum into band-to-band contributions. Such individual band-to-band absorption spectra were then summed up forming two 'partial' absorption spectra that we denote as k_1 and k_2 (Fig. 4, curves 2 and 3, respectively). The first spectrum k_1 comprise band-to-band contributions only from the highest occupied one-electron band to all unoccupied one-electron bands contained between 2 and 5 eV (i.e. to the Ti *d* sub-bands, see Fig. 3). The second absorption spectrum k_2 comprise band-to-band contributions from all one-electron bands located in the upper part of the VB, between −2 and 0 eV to only the lowest Ti *d* sub-band of the CB (from 2 to 3 eV, Fig. 3). It is clearly seen from Fig. 4 that both k_1 and k_2 contribute to formation of the excitation bands in 250–350 nm and 400–470 nm regions. The LBI band of $NaTi_2(PO_4)_3$ emission is excited most effectively in the former region, while the LBII band – in the latter region (Fig. 2, curves 1 and 2). So, we can conclude, that band-to-band transitions which imply transfer of the electronic charge from the oxygen to titanium states are involved into excitation of both emission bands of $NaTi_2(PO_4)_3$ crystals.

The above data allow some general conclusions concerning the origin of luminescence of $NaTi_2(PO_4)_3$ compounds to be drawn. It is

in general associated with centres formed on the basis of the titanium ions. The Ti-related origin should have, first of all, some of the components of the short-wavelength emission band which are excited mainly in region 250–360 nm and the red emission band excited in 425–525 nm region (Figs. 1 and 2). At the same time, the difference in the excitation spectra of these two emission bands suggests that these corresponding emission centres differ substantially. Excitation of the short-wavelength emission band takes place due to transitions from the top of the VB (where the oxygen states dominate) to two narrow sub-bands which originate from unoccupied states of Ti^{4+} ions. Emission of such centres is associated with backward transitions and it is described in literature as emission of Ti^{4+} ions in oxide matrixes. In particular, the 420 nm emission band of Al_2O_3:Ti was assigned to complexes created on the base of closely lying Ti impurities and oxygen vacancies (complex like Ti^{4+}–F-centre [12]). The 460 nm emission band of Al_2O_3:Ti as well as Ti-related 550 nm emission of $Ca_3ZrSi_2O_9$:Ti were ascribed to Ti^{4+} ions [13,14].

Analogous charge transfer processes takes place during excitation of the red emission band of $NaTi_2(PO_4)_3$ compounds. However, in this case stable Ti^{3+} ions in octahedral oxygen coordination are formed. The red emission band of the Ti-doped compounds is usually associated with the Ti^{3+} ions. In particular, emission bands of Al_2O_3:Ti [12] and YAG:Ti^{3+} [15] peaking near 770 nm were attributed to the internal transitions in Ti^{3+} ions. Thus, there is no doubt that the red emission band of $NaTi_2(PO_4)_3$ originate from radiative transitions in Ti^{3+} ions.

So, since the luminescence of $NaTi_2(PO_4)_3$ compounds is related to titanium ions, and the region of effective excitation of both emission bands of $NaTi_2(PO_4)_3$ crystals (excitation into the Ti *d* states) ranges from 300 to 370 nm (Fig. 2), it will be obviously be most convenient to monitor the waste confinement by luminescence excitation in this spectral region. Excitation by the nitrogen laser (λ_{exc} = 337.1 nm) entirely satisfies such a requirement.

Since the short-wavelength emission band of $NaTi_2(PO_4)_3$ crystals is related to emissions from Ti^{4+} (or from Ti^{3+} ions which have a defect in the nearest oxygen surrounding), and the red emission band originate from Ti^{3+} ions which are the defects in host matrix themselves, the changes in concentration ratio of such emitting ions should change intensities, shapes and peak positions of both emission bands. Formation of other types of point defects in the host matrix (e.g. by additional doping) should generate such changes providing essential information concerning the processes of the host matrix emission. On the other hand, additional doping, if it causes new characteristic emission bands, can obviously widen the potential field of application of these compounds for waste confinement. For this purpose subsequent analysis of emission spectra of $NaTi_2(PO_4)_3$ crystals doped with various ions under laser excitation with λ_{exc} = 337.1 nm will be performed.

Disturbance of the oxygen surrounding of the titanium ions should strongly influence characteristics of excitation and emission processes. Alkaline metal ions belong already to the second coordination sphere of the Ti ions, and therefore variations of composition of this region should have less influence on the luminescent properties. The change of the type of M^I cation does not cause significant changes in the PL emission spectra (Fig. 5, a). Shapes and peak positions of both LBI and LBII emissions are almost similar, excluding the case of $LiTi_2(PO_4)_3$ crystal where peak position of LBI is somewhat shifted to lower wavelengths (Fig. 5, curve 1).

The changes in PL spectra become more considerable if ions of indium, aluminum and vanadium which have (or can have) a higher charge are introduced into the host matrix (Fig. 5(b)). Incorporation of the Al ions significantly lowers intensity of LBI band, whereas doping with the In ions cause the decrease of both LBI and LBII emissions (Fig. 5, curves 7 and 8). Peak position of the LBI band of the vanadium doped $KTi_2(PO_4)_3$ crystals is considerably

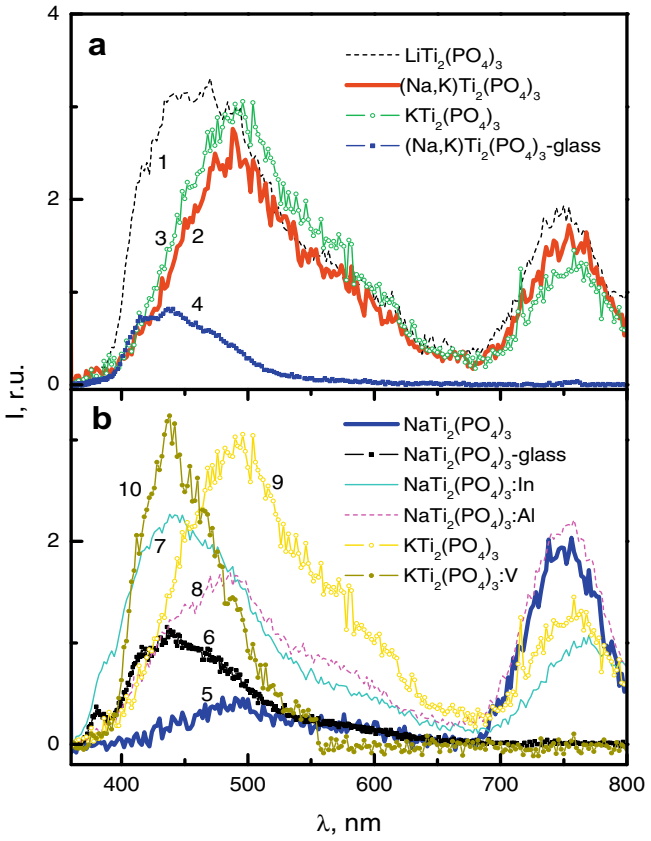

Fig. 5. PL spectra of crystals (1–3, 5, 7–10) and glasses (4, 6):$LiTi_2(PO_4)_3$ (1), $(Na,K)Ti_2(PO_4)_3$, Na/K = 1/3 mass. (2, 4), $KTi_2(PO_4)_3$ (3, 9), $NaTi_2(PO_4)_3$ (5, 6), $NaTi_2(PO_4)_3$:In (7), $NaTi_2(PO_4)_3$:Al (8), $KTi_2(PO_4)_3$:V (10); λ_{exc} = 337.1 nm; *T* = 300 K.

shifted with respect to corresponding peak of undoped crystals, while the red emission band vanishes at all (Fig. 5, curves 9 and 10).

As was noted in the Introduction, we model radiation damage to $M^ITi_2(PO_4)_3$ hosts by considering the amorphous glass-like samples. Fig. 5 shows that emission from such samples differs substantially from emission of their crystalline counterparts (compare curves 2 with 4 and 5 with 6). The most remarkable changes are the absence of LBII bands and the decreasing contributions from long-wavelength components of LBI bands. According to the nature of luminescence clarified above, it can be assumed that destruction of ordering in the crystal matrix is caused by change of stoichiometry during amorphization which probably hampers formation of Ti^{3+} ions. For this reason contribution of their emission decreases and corresponding low-energy components of the short-wavelength emission band diminish.

The rare-earth (RE) ions most probably occupy titanium positions in $M^ITi_2(PO_4)_3$ lattice. It is evident that such situation should predetermine the influence of the RE doping on self emission of host matrixes, and besides this, emission due to transitions in the f shells of RE ions should appear in spectra. Indeed, the RE-doped $NaTi_2(PO_4)_3$ crystals reveal emission bands inherent to RE^{3+} impurities against a background of LBI and LBII emissions (Fig. 6).

The observed groups of narrow lines in the PL emission spectra of crystals doped with Sm^{3+} and Dy^{3+} ions originate from inner f–f electron transitions in the impurity ions (Fig. 6(a) and (c)). The groups of lines in 540–580, 590–625, and 635–670 nm spectral regions (Fig. 6, curve 1) can be ascribed to $^4G_{5/2} \rightarrow {}^6H_{5/2}$, $^4G_{5/2} \rightarrow {}^6H_{7/2}$, and $^4G_{5/2} \rightarrow {}^6H_{9/2}$ transitions in the Sm^{3+} ions, respectively [16,17].

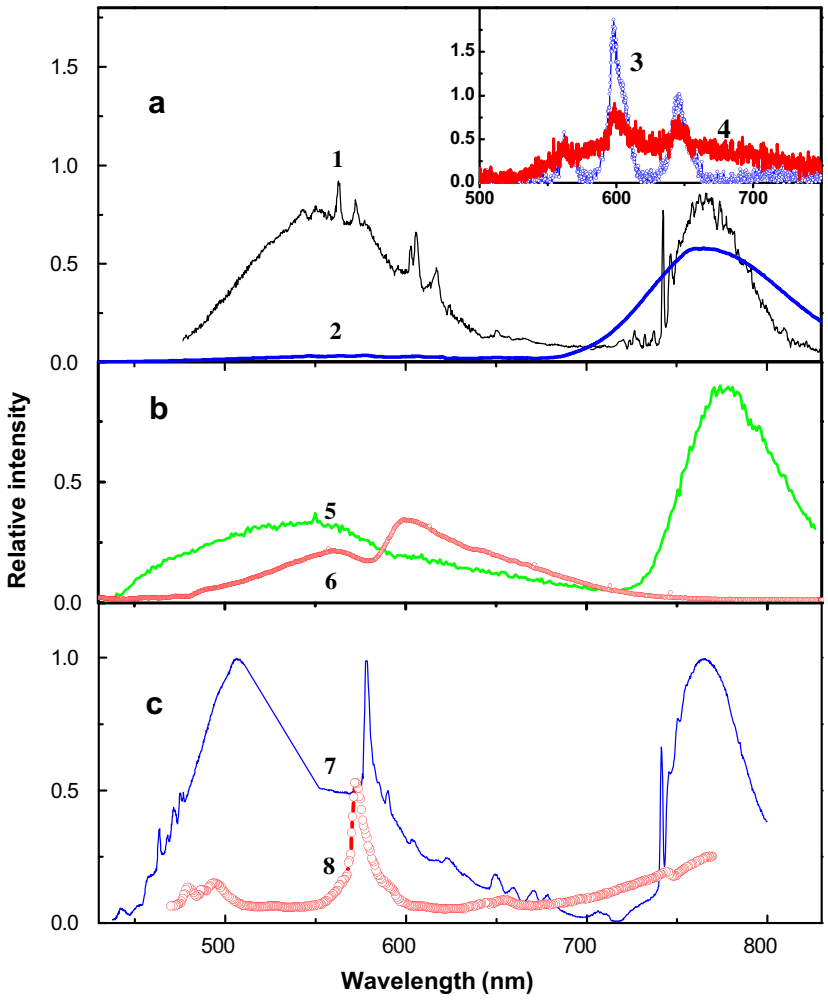

Fig. 6. PL spectra of $NaTi_2(PO_4)_3$ crystals (1–3, 5, 7, 8) and glasses (4, 6) doped with Sm^{3+} (a), Pr^{3+} (b) and Dy^{3+} ions (c); λ_{exc} = 337.1 nm; T = 4.2 (1), 77 (5, 6) and 300 K (2–4, 8).

The PL spectra of $NaTi_2(PO_4)_3$ crystals doped with Pr^{3+} ions also contain both spectral bands of undoped crystals (Fig. 6(b)). The PL spectrum of the glass sample (curve 6) contains only the short-wavelength band which has a complex structure. The shape of the short-wavelength band is distorted and has few details in the green-orange region. The complex character of the spectral bands in this region reveals existence of sub-bands originating from radiative transitions in the impurity Pr^{3+} ions in the crystal as well as in the glass samples. However, no sharp lines corresponding to inner f–f transitions in the Pr^{3+} ions can be clearly observed in the spectra, since the wavelength of applied excitation light (337.1 nm) is not favorable for excitation of luminescence of the Pr^{3+} ions. It is known that there are no inner f–f absorption transitions in the Pr^{3+} ions in a region close to this wavelength [18], in contrast to Sm^{3+} ions being excited directly by such excitation [17].

Emission caused by f–f transitions in the RE ions is most effectively excited via the same f–f transitions (for Sm^{3+} ions, the region of such excitation ranges from 350 to 500 nm, see Fig. 3, curve 3). Therefore, such excitation makes possible observation of the effect of 'crystal-to-glass' structural transition by spectral measurements of f–f emission from the RE dopants. As is clearly seen, amorphization of the host matrix causes weakening of emission bands and their smearing (Fig 6, curves 3 and 4). Thus, we can assert that emission of the RE impurities along with self emission of host matrix can be utilized for detection of the RE ions in $M^{I}Ti_2(PO_4)_3$ hosts, and also for monitoring the structural states of the hosts.

4. Conclusions

(1) Luminescent method is appropriate for: (a) monitoring of incorporation of various types of waste elements (alkaline, transition metal and rare-earth ions) into host matrices of crystal and amorphous phosphates of $MTi_2(PO_4)_3$ type; and (b) observation of changes in structural states of such hosts during long-term waste storage.

(2) The monitoring can be carried out in remote mode with use of laser sources of radiation such as nitrogen laser with generation wavelength 337.1 nm and diode-pumped laser with generation wavelength 473 nm.

(3) Studies of further perspectives and optimization of operation conditions of luminescent monitoring of the $MTi_2(PO_4)_3$ hosts for radioactive waste confinement requires further investigations.

References

[1] G.K. Liu, J.S. Luo, C.-K. Loong, M.M. Abraham, J.V. Beitz, J.K. Bates, L.A. Boatner, Mat. Res. Soc. Symp. Proc. 506 (1998) 921.
[2] K.J. Rao, K.S. Sobha, S. Kumar, Proc. Indian Acad. Sci. (Chem. Sci.) 113 (2001) 497.
[3] R.S. Boyko, O.V. Chukova, O.V. Gomenyuk, P.G. Nagornyi, S.G. Nedilko, Phys. Stat. Sol. (c) 2 (2005) 712.
[4] O. Chukova, S. Nedilko, S. Zayets, R. Boyko, P. Nagornyi, M. Slobodyanik, Opt. Mater. 30 (2008) 684.

[5] Yu. Hizhnyi, O. Gomenyuk, S. Nedilko, A. Oliynyk, B. Okhrimenko, V. Bojko, Radiat. Meas. 42 (2007) 719.
[6] Yu. Hizhnyi, A. Oliynyk, O. Gomenyuk, S. Nedilko, P. Nagornyi, R. Bojko, Opt. Mater. 30 (2008) 687.
[7] P. Blaha, K. Schwarz, G. Madsen, D. Kvasnicka, J. Luitz, *WIEN2k*, An Augmented Plane Wave Local Orbitals Program for Calculating Crystal Properties, Karlheinz Schwarz, Techn. Universitadt Wien, Austria, 2001, ISBN: 3-9501031-1-2.
[8] J.L. Rodrigo, M.P. Carrasko, J. Alamo, Mat. Res. Bull. 24 (1989) 611.
[9] J.P. Perdew, Y. Wang, Phys. Rev. B 45 (1992) 13244.
[10] R.S. Boyko, V.V. Boyko, O.V. Chukova, P.V. Nagornyi, S.G. Nedilko, V.I. Radzivanov, G.I. Gaididei, Funct. Mater. 11 (2004) 147.
[11] Y. Hizhnyi, A. Oliynyk, O. Gomenyuk, S. Nedilko, P. Nagornyi, R. Boiko, V. Boyko, Mater. Sci. Engr. B 144 (2007) 7.
[12] V.B. Mikhailik, H. Kraus, D. Wahl, M.S. Mykhaylyk, Appl. Phys. Lett. 86 (2005) 101909.
[13] W.C. Wong, D.S. McClure, S.A. Basun, M.R. Kokta, Phys. Rev. B 51 (1995) 5682.
[14] Aierken Sidike, I. Kusachi, N. Yamashita, Phys. Chem. Minerals 32 (2006) 665.
[15] F. Bantein, P. Albers, G. Huber, J. Lumin. 36 (1987) 363.
[16] M.J. Treadaway, R.C. Powell, Phys. Rev. B 11 (1975) 862.
[17] O. Chukova, S. Nedilko, Z. Moroz, M. Pashkovskyi, J. Lumin. 102&103 (2003) 498.
[18] S.G. Nedilko, M. Diab, L.M. Limarenko, Z.T. Moroz, M.V. Pashkovskyi, Ukrain. Phys. J. 42 (1997) 415.